

# **CAN FIELD WIDE VARIATIONS IN WATER INJECTIVITY DURING WAG BE EXPLAINED BY DIFFERENCES IN ROCK TYPE?**

Jairam Kamath and Frank Nakagawa, ChevronTexaco

## **ABSTRACT**

Some injectors in the McElroy field in West Texas have experienced drastic reduction in chase brine injectivity during the Water-Alternating-Gas (WAG) process. We conducted laboratory corefloods on different rock types selected from good and poor injectors to investigate potential causes. We found that there was insufficient difference in the responses of the different rock types to explain water injectivity differences in the field. The chase brine injectivity was comparable to the secondary waterflood injectivity. It increased significantly with dissolution of the trapped CO<sub>2</sub>. The CO<sub>2</sub> injectivity was substantially larger than the secondary waterflood injectivity.

Unable to explain field-wide variations in injectivity with these corefloods, we investigated whether poor local sweep could lead to reduced injectivity. Dripping of bypassed oil into a thin high permeability CO<sub>2</sub> channel could cause plugging due to asphaltene deposition. This could then lead to injectivity loss in the subsequent water cycle. We designed an experiment where we "soaked" a core with slugs of crude oil (to represent dripping of bypassed oil) and CO<sub>2</sub>. A subsequent waterflood led to reduced injectivity. These results suggest that two necessary conditions for injectivity loss are poor sweep and precipitation of a heavy phase.

## **INTRODUCTION**

Injectivity has a direct impact on project economics, and loss of injectivity in WAG projects is an area of concern. Experience to date has been that most projects will experience some loss of injectivity during the water injection cycle of the WAG process, with the average being about 20%.<sup>1</sup> However, there have been cases reported where the loss of water injectivity has been severe.<sup>2</sup> Also, lower than anticipated CO<sub>2</sub> injectivity has been observed in a number of field trials. This seems to be particularly true in the low temperature carbonate reservoirs of West Texas.<sup>3,4</sup>

Amoco reported results of four field projects using alternate rich-gas and water injection.<sup>2</sup> In one project, a San Andres dolomite West Texas flood, the water injectivity was a factor of three lower than that measured prior to any gas injection. The other projects experienced no loss in injectivity. The West Texas project had lower permeability rocks, more viscous and asphaltic oil, and more anhydrite. In order to understand the results of the field projects, Amoco conducted ambient condition laboratory tests using model fluids on 19 carbonate samples from four reservoirs.<sup>5</sup> It does not appear that they found any differences between responses of the rocks from the different reservoirs. They concluded that the reduced water injection was due to the presence of residual oil to miscible flooding; and conjectured that the asphaltic West Texas oil caused large

residuals. Texaco found that the water injectivity in a field trial in the San Andres formation was significantly greater than the pre-CO<sub>2</sub> waterflood injectivity.<sup>6</sup> Reservoir condition laboratory work on four core samples showed that dissolution of trapped CO<sub>2</sub> caused large increases in water injectivity. Phillips Petroleum has recently reported reservoir condition laboratory data on two dolomite core samples from the South Cowden field in West Texas.<sup>7</sup> The injectivity of CO<sub>2</sub> saturated brine was reduced by a factor of two to three in their tests.

### **Current Work**

This study reports on our efforts to understand why some wells in the McElroy field, West Texas, experienced drastic losses in water injectivity whereas others did not. We first report on our conventional coreflood data, and then on a coreflood on a "soaked" core designed to mimic high local heterogeneity.

#### Conventional corefloods

We designed a program that investigates the injectivity of the major zones during a WAG process – secondary waterflood, oil bank, solvent, chase water with trapped gas and residual oil saturation, and chase water with trapped oil saturation. We conducted our measurements in liquid CO<sub>2</sub>-water, liquid CO<sub>2</sub>-water-toluene, and liquid CO<sub>2</sub>-water-crude systems. This allowed us to understand the mechanisms for the loss, and to evaluate the wettability related issues raised because we had to work with old cores. The tests were conducted on several different rock types selected from a good injector and a poor injector.

#### Coreflood on "soaked" core

Unable to explain the field wide variations in injectivity with our corefloods, we investigated whether poor injectivity was caused by poor local sweep. Continuous dripping of bypassed oil into a high permeability CO<sub>2</sub> channel could cause plugging due to asphaltene deposition. This would then lead to injectivity loss in the subsequent water cycle. We designed an experiment where we "soaked" a core with slugs of crude oil (to represent bypassed oil) and CO<sub>2</sub>.

## **CONVENTIONAL COREFLOODS**

### **Zones in WAG flood**

Figure 1 shows five idealized zones present during a WAG process. The water zone corresponds to the secondary waterflood and contains residual oil to waterflood,  $S_{orw}$ . The oil zone is the miscible oil bank displacing water. The CO<sub>2</sub> rich phase zone consists of CO<sub>2</sub> displacing residual oil and water. The chase water corresponds to the water cycle in the WAG process and consists of two zones. One zone has trapped CO<sub>2</sub>,  $S_{CO_2t}$ , and residual oil to miscible flood,  $S_{orm}$ . The chase water zone closest to the injector, INJ, contains only  $S_{orm}$  as the water has dissolved the trapped CO<sub>2</sub>.

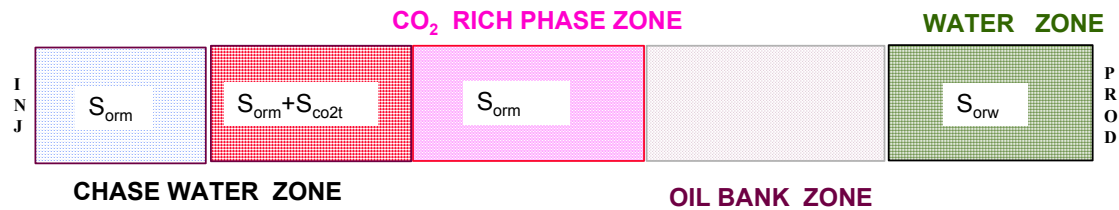


**Figure 1.** Idealized zones during a WAG process.

The overall injectivity during WAG is the distance-weighted function of the injectivities of the different zones. Our experimental approach is based on measuring the injectivities of these zones as a function of pore volumes throughput. This is similar to other studies.<sup>5,6,7</sup> We did not study overall injectivities using small alternate slugs of CO<sub>2</sub> and water because it does not mimic near well bore flow through patterns. The small slug method is common for studying residual oil saturation to WAG,<sup>3</sup> but does not appear to have been used for injectivity studies.

### Sample Selection

We selected 21 samples from a poor injector and 22 samples from a producer offsetting a good injector. These samples had not been preserved and were chosen to cover a range of rock types. We miscibly cleaned these samples with alternating flushes of toluene and methanol; measured the methanol permeability; vacuum dried the samples; measured porosity and air permeability; and finally measured trapped gas saturation by immersing dry samples in toluene. We used this data and visual inspection to classify the rocks into the four types shown in Table 1. The samples in *Italics* are from the poor injector. The shaded samples in each rock type were combined to form composite core samples and used in the injectivity tests.

### Procedures

We used the following procedures for the injectivity tests. A schematic of the experimental set-up is at the end of this paper.

1. Start with brine saturated core samples.
2. Displace with liquid CO<sub>2</sub> at fixed rate. Raise rate at end of tests to measure incremental production and change in CO<sub>2</sub> permeability.
3. Flood with CO<sub>2</sub> saturated brine at low rate.
4. Follow with unsaturated brine at low rate.
5. Displace with toluene at low flow rate until brine production ceases. Raise pressure drop in steps until there is no more incremental brine production.
6. Brine flood at initial rate\* (typically 1 ml/minute). Raise rate (to typically 5 ml/minute) at end of tests to measure incremental production and change in brine permeability. Pore volume of core ~ 30 ml.

\* rates chosen to correspond to flow rates in the near well region; rate bumps used to gage importance of flow rates on end-point data

7. Flood with liquid CO<sub>2</sub> at low rate. Raise rate at end of tests to measure incremental production and change in CO<sub>2</sub> permeability.
8. Flood with CO<sub>2</sub> saturated brine at low rate.
9. Flood with unsaturated brine at low rate.
10. Displace brine-saturated sample with toluene and replace with crude. Age the sample for a minimum of three days (typically one week) at reservoir temperature (88 degF) and pressure (2000 psi).
11. Repeat steps 6 to 10 at reservoir temperature and pressure.

**Table 1.** Properties of rock samples representing the range of rock types in the McElroy field CO<sub>2</sub> pilot area.

ROCK TYPE	por (%)	Ka (md)	K liq (md)	Sgt (%)
good quality moldic	15.5	59		
	15.7	34	45	33
	15.9	29		43
	13	10	29	30
	14.8	12		
good quality fine inter-crystalline	16.1	17	29	24
	18.4	35	42	24
	15.9	29	31	29
	16.6	35		40
	16.6	49	66	30
medium quality moldic	15.9	22	12.7	
	16.6	35	5.4	
	14	19		
	15.3	23	6.7	
	15.9	25	4.2	
	13.1	26		
	14.8	19		
	13.2	7.5	11	38
	15.1	8.4	11	26
	14.4	12	8.4	25
	17.4	8.8	6.4	
	15.6	18	6.4	
poor quality	7.8	0.62	0.03	
	10.9	21	0.46	
	10.6	11	0.37	
	9.3	5.6	0.15	
	14.6	6.9	3.5	28
	11	1.8	0.34	24
	10.3	6.6	2	
	13.5	6.7	2.5	30
	14.2	5.2	2.5	
	12.8	0.75	0.21	
13.7	3.1	2.8		
14.2	8.8	5	23.6	

### Crude Oil Properties

Stock tank oil was blended with synthetic gas to prepare the 32° API crude oil sample.

The bubble point of the oil is 221 psi at the reservoir temperature of 88 deg F. Table 2 displays the results of compositional analysis of the crude sample. This oil is very similar to the crude samples studied by Creek and Sheffield,<sup>8</sup> and extensive phase behavior information is reported in their work.

**Table 2.** Crude Oil Analysis

Component	Mole %	Component	Mole %	Component	Mole %
N <sub>2</sub>	0.54	C <sub>6</sub>	4.02	C <sub>16</sub>	2.35
CO <sub>2</sub>	0.59	C <sub>7</sub>	8.65	C <sub>17</sub>	2.41
C <sub>1</sub>	4.15	C <sub>8</sub>	6.23	C <sub>18</sub>	2.01
C <sub>2</sub>	3.10	C <sub>9</sub>	6.53	C <sub>19</sub>	1.65
C <sub>3</sub>	4.32	C <sub>10</sub>	5.19	C <sub>20</sub>	1.49
iC <sub>4</sub>	0.96	C <sub>11</sub>	4.24	C <sub>21</sub>	1.33
nC <sub>4</sub>	3.49	C <sub>12</sub>	3.75	C <sub>22</sub>	1.21
iC <sub>5</sub>	2.26	C <sub>13</sub>	3.60	C <sub>23</sub>	1.11
nC <sub>5</sub>	2.53	C <sub>14</sub>	3.11	C <sub>24</sub>	0.94
		C <sub>15</sub>	2.77	C <sub>25+</sub>	15.47

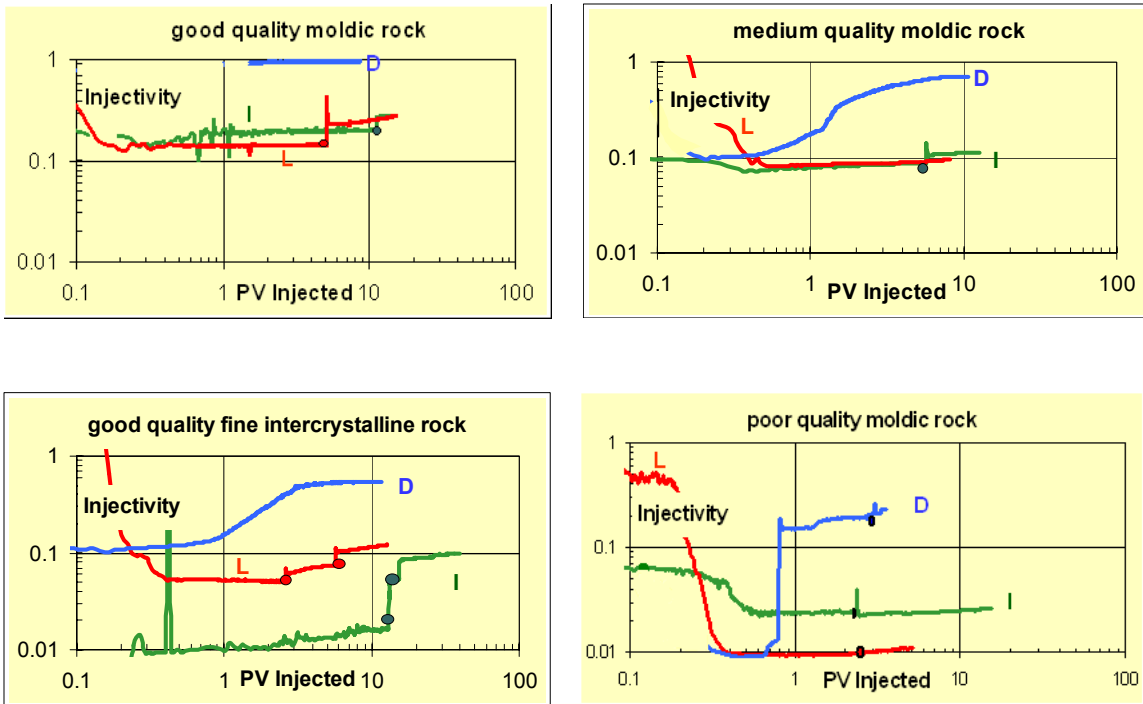
### Experimental Data

Injectivity is defined as the ratio  $\frac{(q / \Delta P)}{(q / \Delta P)_{\text{single phase brine}}}$ . Viscosity of the brine is 1 cP, that of the crude is 4.5 cP, and that of CO<sub>2</sub> is 0.08 cP.

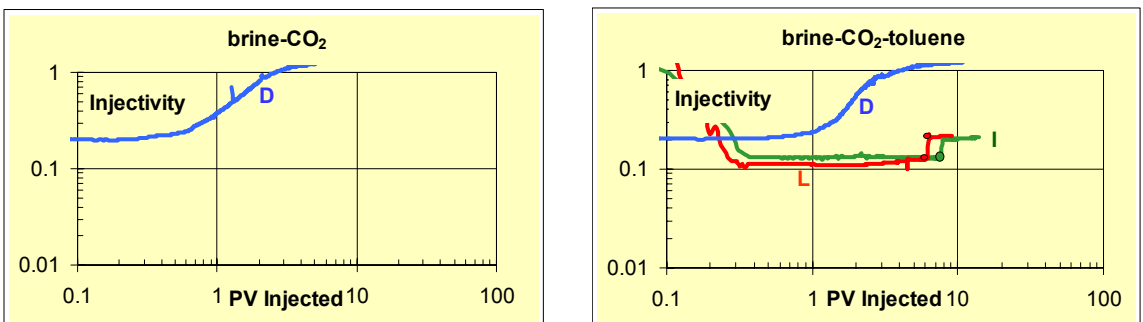
#### Water Injectivity

Figure 2 contains the water injectivity data for the liquid CO<sub>2</sub>-water-crude system. Brine injectivity after CO<sub>2</sub> (live brine flood -- L) is comparable to the secondary waterflood (I) injectivity and increases significantly as trapped CO<sub>2</sub> dissolves (dead brine flood -- D). The solid circles (●) correspond to flow rate increases from 1 cc/minute to 5 cc/minute. Flow rate increases have small effects except for the good quality fine intercrystalline rock. The secondary waterflood injectivity is unstable in this case, possibly due to problems with crude oil plugging<sup>9</sup> during the establishment of initial water saturation.

Figure 3 shows that the brine-liquid CO<sub>2</sub> and brine-liquid CO<sub>2</sub>-toluene gave similar response to the liquid CO<sub>2</sub>-crude-brine system. The data is for the good quality moldic rock system and is typical for all rock types. We had to work with unpreserved cores, and this alleviates concerns that wettability may be a key factor in explaining differences in brine injectivity.



**Figure 2.** Chase live brine (L) and chase dead brine (D) injectivity is equal or greater than the secondary waterflood (I) injectivity. Brine-liquid CO<sub>2</sub>-crude system.



**Figure 3.** Brine injectivity data for the brine-liquid CO<sub>2</sub> and brine-liquid CO<sub>2</sub>-toluene systems. Good quality moldic rock. I = secondary waterflood; L = live brine flood; D= dead brine flood.

CO<sub>2</sub> Injectivity

Figure 4 reveals that the CO<sub>2</sub> injectivity rapidly climbs above the secondary waterflood injectivity (.02-.2). The CO<sub>2</sub> floods were carried out after the secondary waterflood; The solid circles (●) correspond to flow rate increases.

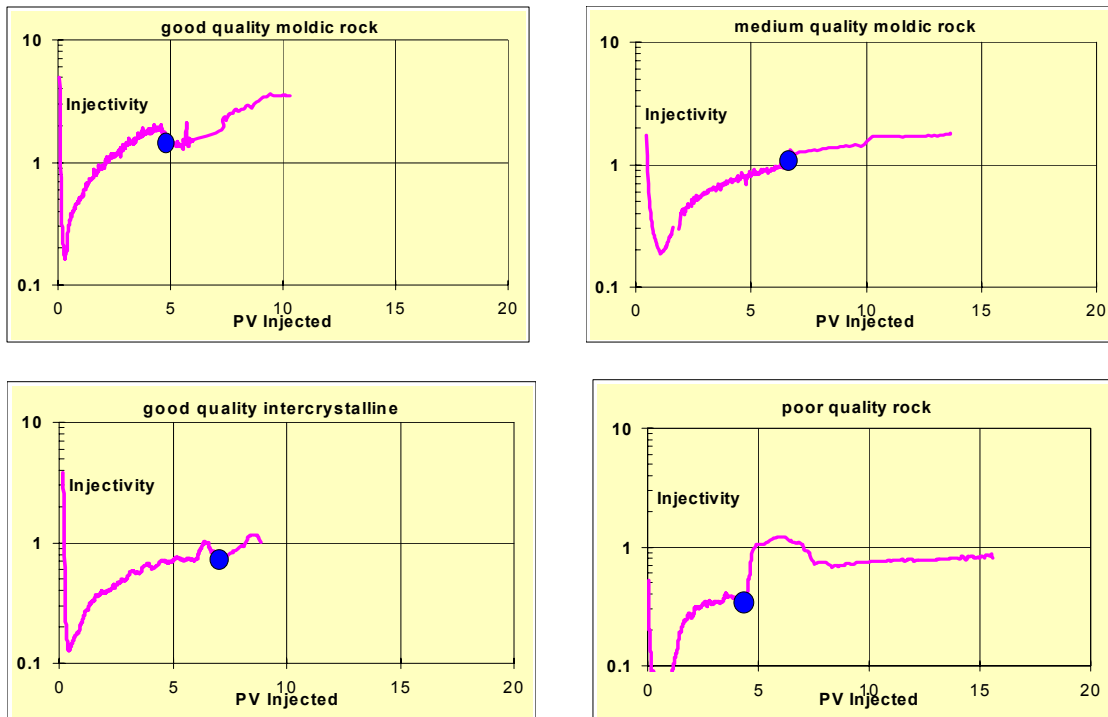


**Figure 4.** CO<sub>2</sub> injectivity as function of pore volumes injected. Brine-liquid CO<sub>2</sub>-crude system.

#### End Point Injectivity Data

Figure 5 summarizes the end point injectivity data for the different zones in a WAG process. The CO<sub>2</sub> end point injectivity is often ill-defined, as CO<sub>2</sub> injectivity often continued to increase with throughput and after measurable liquid production had stopped. The water zone (oil saturation =  $S_{orw}$ ) has low injectivities of around 0.15. This is similar to values obtained by other investigators on comparable dolomites.<sup>5,7,13</sup> There is no systematic difference between the cleaned state ambient condition tests and the restored state reservoir condition tests.

The CO<sub>2</sub> rich phase zone has higher injectivities than the water zone, and is in agreement with earlier work.<sup>6,7</sup> The highest injectivity is for the good quality fine intercrystalline rock with toluene as the oil phase; and the lowest injectivity is for the poor quality rock with crude as the oil phase. The chase water zone with trapped CO<sub>2</sub> has injectivities comparable to the secondary waterflood. Earlier studies<sup>5-7</sup> on San Andres dolomites have found anything from comparable to much lower injectivities of the chase water zone. The injectivity of the chase water zone rises rapidly with dissolution of the CO<sub>2</sub>. This agrees with the findings of the only other study that has looked at this zone.<sup>6</sup> The toluene system has slightly better injectivity values than the crude system.

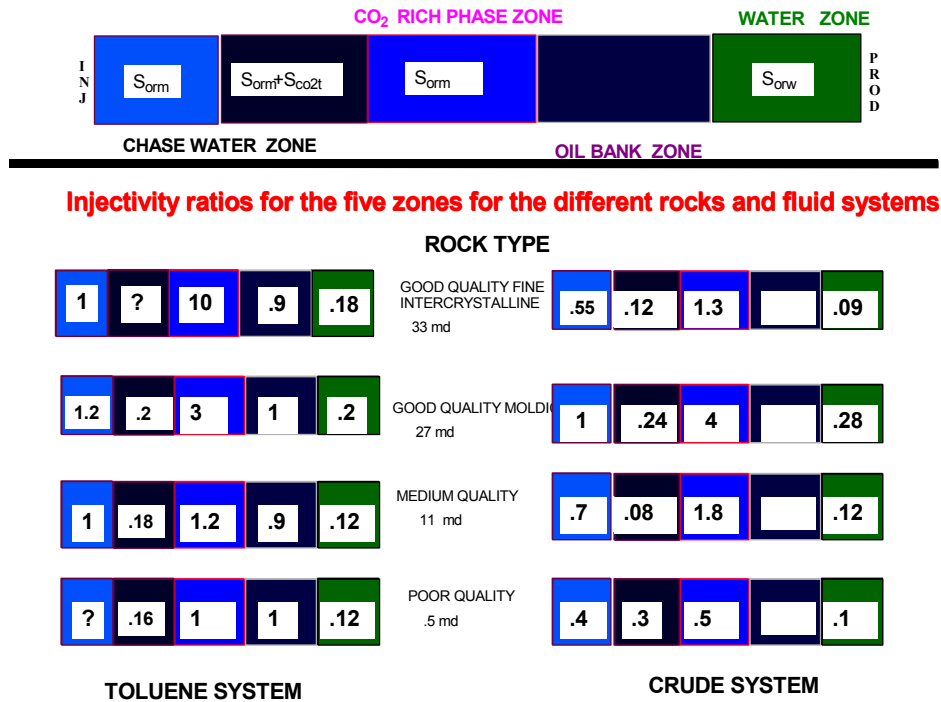


**Figure 5.** End point injectivity ratios for the different rocks and oil systems. The data is normalized to injectivity of single phase water.

Discussion

The primary objective of this study was to understand why some wells in McElroy field experienced drastic losses in water injectivity whereas others did not. The good quality moldic and medium quality moldic rocks represent the higher permeability rock type for the good injector and poor injector respectively. The good quality fine intercrystalline and poor quality rocks represent the corresponding lower permeability rocks for these wells. We do not notice significant differences in water injectivity behavior between these sets of rocks. We find that live chase brine gives injectivity values similar to the secondary waterflood. Dead brine injectivity rises to unity with dissolution of the trapped CO<sub>2</sub>, in agreement with the data of Prieditis et. al.<sup>6</sup> This implies that CO<sub>2</sub> has been effective in reducing oil saturation in the main water flow path. The near well bore environment is subject to though put of many pore volumes of each fluid. Therefore, it is reasonable to expect that during the water cycle we are in a condition with low residual oil and little trapped gas. The water mobility in this region should be high.

**FLOODS ON "SOAKED" CORES**

We have so far been unable to explain differences in water injectivity due to differences in rock types. In fact, our data seems to suggest that water injectivity following CO<sub>2</sub> flooding should continue to improve.



We studied the logs from a good injector and a poor injector and found that the permeability patterns were significantly different. The good injector had thicker zones of high permeability; zones containing permeability greater than 1 md is shown in figure 6.

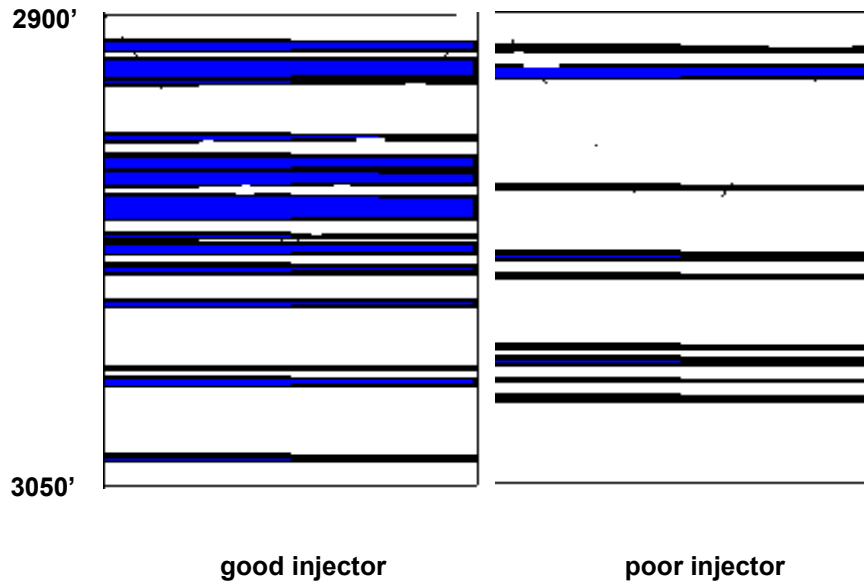


**Figure 6.** The good injector has thicker zones of high permeability. Shaded regions contain permeability greater than 1 md.

This finding led to a hypothesis that poor local sweep during the secondary waterflood is a precursor for subsequent injectivity problems. Elements of this hypothesis are -- initial waterflood penetrates the better quality rocks; CO<sub>2</sub> follows this path; this CO<sub>2</sub> channel is obstructed if the channel is thin and there is a large source of bypassed oil that drips into it; and subsequent water injectivity is low if the CO<sub>2</sub> channel is obstructed. The CO<sub>2</sub> channel is obstructed in our situation because of asphaltene precipitation.<sup>8</sup> This mechanism is illustrated in figure 7.

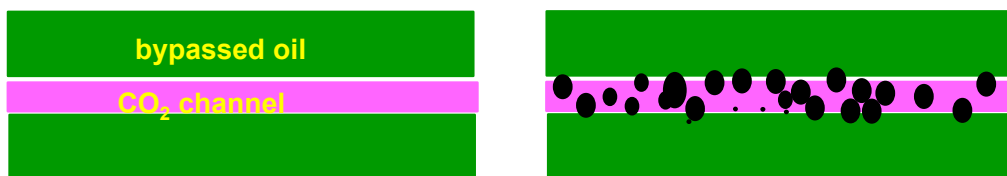


**Figure 7.** Potential mechanism of water injectivity loss caused by poor local sweep and bypassed oil dripping into main flow channels.

We decided to test the above hypotheses by conducting a coreflood on a "soaked" core. The mechanism of bypassed oil dripping into the CO<sub>2</sub> channel was modeled by injecting alternating slugs of CO<sub>2</sub> and crude into the core, and allowing the core to "soak" before waterflooding. It is well documented that asphaltenes precipitate when the CO<sub>2</sub> and the oil mix, and the period of marination allows sufficient contact time to allow asphaltenes

to precipitate. In conventional corefloods, asphaltenes can only deposit at the leading edge of the front, and there is insufficient time for significant deposition.

### Experimental Data

We used the medium quality moldic core sample and crude oil described in the section on conventional corefloods. After saturating and aging the core sample with crude oil at initial water saturation, we injected alternating slugs of 0.03 PV of CO<sub>2</sub> and crude into the core. This was continued until we had injected 0.7 PV each of CO<sub>2</sub> and crude. The core was then shut in for 3 weeks and allowed to "soak". CO<sub>2</sub> saturated brine was then injected into the core at 0.1 cc/minute and followed by dead brine at the same flow rate. Figure 8 shows that the brine injectivity is significantly reduced. End point injectivity values are 0.04 and 0.3 for the live and dead brines respectively. For comparison, the corresponding end point injectivity on the "non-soaked" medium quality moldic rock were 0.1 and 0.7.

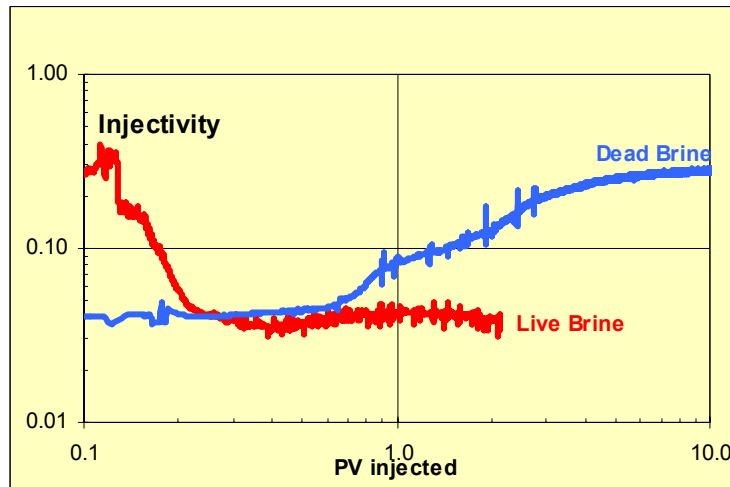


**Figure 8.** Injectivity data for a live brine flood followed by a dead brine flood. Medium quality moldic "soaked" core.

### CONCLUSIONS

Conventional coreflood data did not yield significant difference in injectivity response between the rock types present near a poor injector and those present near a good injector. Chase brine injectivity was comparable to the secondary waterflood injectivity, and increased significantly with dissolution of the trapped CO<sub>2</sub>. The CO<sub>2</sub> injectivity was substantially larger than the secondary waterflood injectivity. The injectivity of the chase water and CO<sub>2</sub> zones was a weak function of whether cleaned or restored state samples were used.

Floods on cores "soaked" with alternating slugs of CO<sub>2</sub> and crude showed more than a factor of two initial reduction in the chase brine injectivity. It is possible that such corefloods are necessary to investigate injectivity reductions in the field. Our results suggest that two necessary conditions for injectivity loss are poor sweep and precipitation of a heavy phase.

## ACKNOWLEDGMENTS

We thank Kelly Edwards for his active support and involvement with this project; and Leon Roe and Mitch Harris for core selection and geological classification.

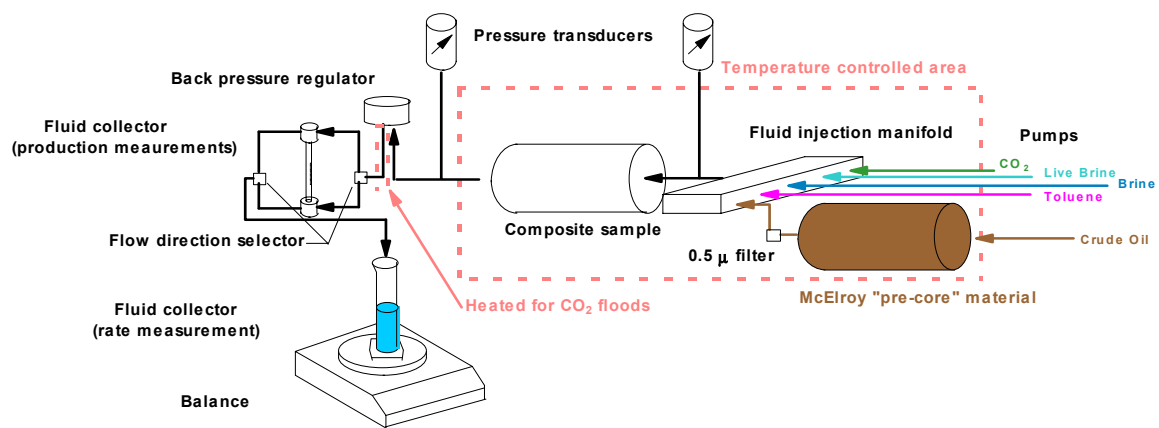
## NOMENCLATURE

- PV = pore volumes
- $\Delta P$  = pressure drop, psi
- q = flow rate, cc/min
- S<sub>orw</sub> = residual oil saturation to secondary waterflood, %
- S<sub>orm</sub> = residual oil saturation to miscible CO<sub>2</sub> flood, %
- S<sub>co2t</sub> = trapped CO<sub>2</sub> saturation, %
- S<sub>gt</sub> = trapped gas saturation, %
- S<sub>wi</sub> = initial water saturation, %

## REFERENCES

1. Hadlow, R. E. "Update of Industry Experience with CO<sub>2</sub> flooding," SPE 24928 presented at the 67<sup>th</sup> Annual Technical Conference and Exhibition, Washington, DC, October 4-7, 1992.
2. Harvey, M. T., Shelton, J. L., and Kelm, C. H.: "Field Injectivity Experiences with Miscible Recovery Projects Using Alternate Rich-Gas and Water Injection," JPT September 1977 p1051-1055.
3. Stalkup, F. I., Jr.: Miscible Displacement, SPE Monograph Series v8 1983 p. 155.
4. Rogers, J. D. and Grigg, R. B. "A Literature Analysis of the WAG Injectivity Abnormalities in the CO<sub>2</sub> process," SPE Reservoir Evaluation and Engineering October 2001
5. Schneider, F. N. and Owens, W. W.: "Relative Permeability Studies of Gas-Water Flow Following Solvent Injection in Carbonate Rocks," SPEJ February 1976 pp 23-30.
6. Prieditis, J., Wolle, C. R., And Notz, P. K.: "A Laboratory and Field Injectivity Study: CO<sub>2</sub> WAG in the San Andres Formation of West Texas," SPE 22653 presented at the 68<sup>th</sup> Annual Technical Conference and Exhibition, Dallas, TX, October 6-9, 1991.
7. Wegener, D. C. and Hapole, K. J.: "Determination of Relative Permeability and Trapped gas Saturation for Predictions of WAG performance in the South Cowden CO<sub>2</sub> Flood," SPE/DOE 35429 presented at the 1996 SPE/DOE Tenth Symposium on Improved Oil Recovery, Tulsa, OK, 21-24 April 1996.

8. Creek, J. L. and Sheffield, J. M. "Phase Behavior, Fluid Properties, and Displacement Characteristics of Permian Basin Reservoir Fluid/CO<sub>2</sub> systems," SPERE February 1993.
9. Kamath, J. et. al.: "Laboratory Investigation of Injectivity Losses During WAG in West Texas Dolomite," SPE 39791 presented at the 1998 SPE Permian Basin Oil and Gas Recovery Conference, Midland, Texas, 25–27 March 1998.



Schematic of Experimental Set-up